HNPS Advances in Nuclear Physics

Vol 32 (2026)

HNPS2025

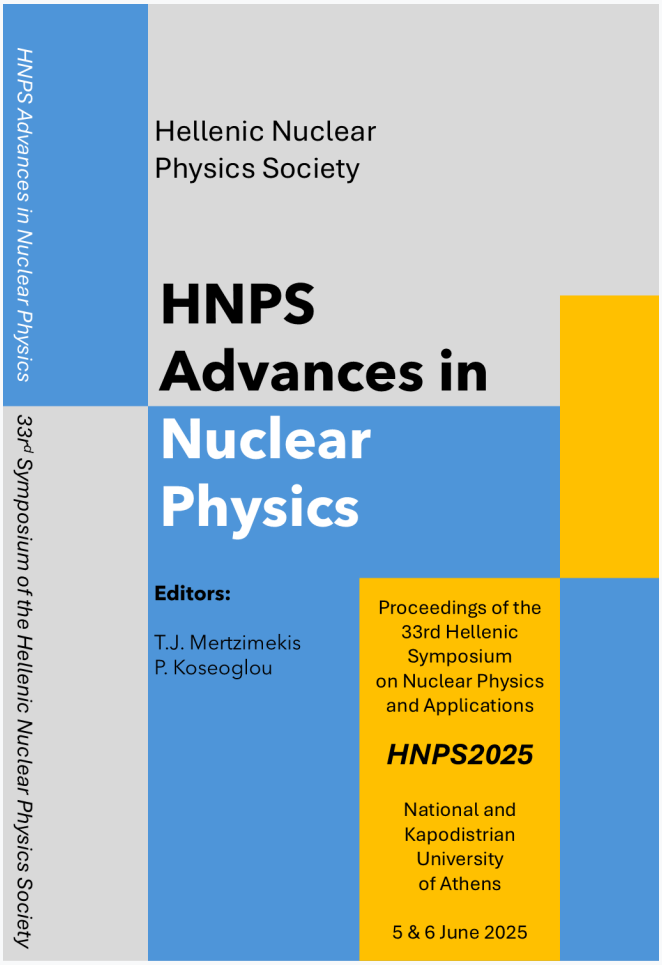

Shape transitions and collective behaviour of Er and Yb isotopes based on relativistic energy density functional theory

Konstantinos Karakatsanis, Theo J. Mertzimekis, Pavlos Koseoglou

doi: 10.12681/hnpsanp.8896

To cite this article:

Karakatsanis, K., Mertzimekis, T. J., & Koseoglou, P. (2026). Shape transitions and collective behaviour of Er and Yb isotopes based on relativistic energy density functional theory. *HNPS Advances in Nuclear Physics*, *32*, 32–41. https://doi.org/10.12681/hnpsanp.8896

HNPS Advances in Nuclear Physics Vol. **32**, 32–41 (2025)
doi: 10.12681/hnpsanp.8896

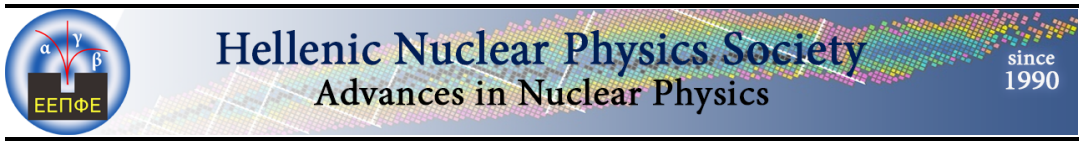

ARTICLE

Shape transitions and collective behaviour of Er and Yb isotopes based on relativistic energy density functional theory

K.E. Karakatsanis,[*,1] T.J. Mertzimekis,[2] and P. Koseoglou[2]

[1]Institute of Nuclear and Particle Physics, National Centre for Scientific Research "Demokritos", GR-15310 Aghia Paraskevi, Attiki, Greece
[2]Department of Physics, National and Kapodistrian University of Athens, Zografou Campus, GR-15784 Athens, Greece
*Corresponding author: kokaraka@hotmail.com

(Received: 09 Nov 2025; Accepted: 23 Nov 2025; Published: 25 Nov 2025)

Abstract
In this work a collective Hamiltonian based on relativistic energy density functional calculations has been used to study the basic spectroscopic properties of Er and Yb isotopes with $82 < N < 114$. Starting from a series of shape constrained calculations, we build a Bohr-type Hamiltonian the diagonalisation of which gives the collective excitations and transition probabilities. We are thus able to follow the transition of shapes, which is established through projected energy surfaces and specific spectroscopic quantities such as energy ratios and the structure of the low lying excited states.

Keywords: Nuclear structure theory; Relativistic density functionals; Shape transitions

1. Introduction

Medium heavy nuclei in the lanthanide region of the periodic table are in constant focus of precise experimental efforts, in order to accurately pinpoint the standard characteristics of transitional nuclei. The change in shape of even-even Erbium and Ytterbium nuclei along the neutron-rich side of their isotopic chains, from $N = 82$ to $N = 110$, is such a case. Very recent experiments have been performed by the nuclear physics group of NKUA at IFIN-HH Bucharest, in a number of Yb isotopes, results of which are reported in another contibution by Dr. P. Koseoglou in the current issue of HNPS Advances in Nuclear Physics. In this, a theoretical study is presented using the relativistic energy density functional framework and its extension beyond the mean-field level. The starting point is a Lorentz- invariant Lagrangian that defines an effective interaction via the exchange of virtual mesons, coupled to the nucleon wavefunction [1–3]. In this framework, nucleons are treated as Dirac spinors. Since the nuclei under investigation are mainly open-shell, an additional finite-range separable pairing force in momentum space is included [4, 5]. By appropriately defining the particle

 ISBN 2654-007X (print), 2654-0088 (online).

and pairing densities, a covariant energy density functional is constructed, the variation of which leads to the Relativistic Hartree-Bogoliubov (RHB) equations [6]. These equations are solved using the DIRHB code in a triaxial basis, allowing for quadrupole degrees of freedom described by the β_2 and γ deformation parameters [7]. By imposing constraints on these variables during the solution of the RHB equations, potential energy surfaces are obtained for each isotope. The ground-state shape is identified with the global minimum of the surface. Following this procedure, the evolution from spherical to well-deformed axially symmetric shapes is illustrated for both isotopic chains

In a second step, a five-dimensional collective Hamiltonian incorporating vibrational and rotational degrees of freedom is constructed [8]. Its parameters are determined from the Bogoliubov quasi-particle wavefunctions and occupation numbers obtained from the constrained RHB calculations. Diagonalization of the collective Hamiltonian yields the low-lying collective excitation spectra and $E2$ transition probabilities. Examining the ratios of these observables provides important insights into the collective behavior of the isotopes under investigation.

2. Theoretical Framework

2.1 Relativistic energy density functional

The theoretical modeling of nuclear structure phenomena requires a sophisticated application of one of several quantum many body problem methods [9]. Energy density functionals is one of the most powerful and successful tool that allows a universal study of the most important nuclear physical properties. The starting point is a Lagrangian density function with a minimal set of degrees of freedom necessary for the description of the nucleon nucleon interaction. In the case of relativistic mean field theory [1], where nucleons are treated as Dirac spinors that interact via the exchange of virtual mesons this Lagrangian consists of three parts

$$\mathcal{L} = \mathcal{L}_N + \mathcal{L}_m + \mathcal{L}_{int.} \tag{1}$$

The first part describes the free motion of Dirac spinors

$$\mathcal{L}_N = \bar{\psi}(i\gamma_\mu\partial^\mu - m)\psi, \tag{2}$$

the second part contains the free mesons and photon terms

$$\mathcal{L}_m = \frac{1}{2}\partial_\mu\sigma\partial^\mu\sigma - \frac{1}{2}m_\sigma^2\sigma^2 - \frac{1}{2}\Omega_{\mu\nu}\Omega^{\mu\nu} + \frac{1}{2}m_\omega^2\omega_\mu\omega^\mu - \frac{1}{4}\vec{R}_{\mu\nu}\vec{R}^{\mu\nu} + \frac{1}{2}m_\rho^2\vec{\rho}_\mu\vec{\rho}^\mu - \frac{1}{4}F_{\mu\nu}F^{\mu\nu}, \tag{3}$$

and the last part includes the minimal set of interaction terms

$$\mathcal{L}_{int.} = -g_\sigma\bar{\psi}\psi\sigma - g_\omega\bar{\psi}\gamma^\mu\psi\omega_\mu - g_\rho\bar{\psi}\vec{\tau}\gamma^\mu\psi\vec{\rho}_\mu - e\bar{\psi}\gamma^\mu\psi A_\mu. \tag{4}$$

In this picture three mesons are used to simulate the nuclear interaction. The sigma meson: an isoscalar scalar field responsible for the long range attraction. The omega meson: an isoscalar vector field responsible for the short range repulsion. The rho meson: an isovector vector field responsible for the isospin dependence. In addition to that the electromagnetic field is also included with the vector potential A^μ. Based on the respective densities $\rho_s(\mathbf{r})$, $j_\mu(\mathbf{r})$, $\vec{j}_\mu(\mathbf{r})$ and $j_{em}(\mathbf{r})$, we can write the Hamiltonian density as follows:

$$\begin{aligned}\mathcal{H}(\mathbf{r}) = &\sum_i^A \psi_i^\dagger(\alpha\mathbf{p} + \beta m)\psi_i + \frac{1}{2}[(\nabla\sigma)^2 + m_\sigma^2\sigma^2] - \frac{1}{2}[(\nabla\omega)^2 + m_\omega^2\omega^2] - \frac{1}{2}[(\nabla\rho)^2 + m_\rho^2\rho^2] - \frac{1}{2}[(\nabla A)^2] \\ &+ [g_\sigma\rho_s\sigma + g_\omega j_\mu\omega^\mu + g_\rho\vec{j}_\mu\cdot\vec{\rho}^\mu + e j_{em}A^\mu].\end{aligned} \tag{5}$$

Finally the energy density functional comes from the integration of the Hamiltonian density over the coordinate space

$$E_{RMF}[\psi, \bar{\psi}, \sigma, \omega^{\mu}, \vec{\rho}^{\mu}, A^{\mu}] = \int d^3\mathcal{H}(\mathbf{r}). \tag{6}$$

A crucial component for the accurate description of nuclei located in the middle of a nucleonic shell is the inclusion of pairing correlations. The natural extension of the above picture is the Relativistic Hartree- Bogoliubov (RHB) approach. The basic concept is the transformation from particle to quasiparticles using the pair creation and annihilation operators,

$$\alpha_k^{\dagger} = \sum^{n} U_{nk} c_n^{\dagger} + V_{nk} c_n, \tag{7}$$

defined from the usual particle creation $c_n^{\dagger}$ and annihilation c_n operators. In the RHB approach the ground state defines the quasiparticle vacuum i.e. $\alpha_k|\Phi\rangle = 0$ for $E_k > 0$ or $|\Phi_0\rangle = \prod_{E_k>0} \alpha_k|-\rangle$. Aside from the normal particle density $\hat{\rho}_{nn'} = \langle\Phi|c_{n'}^{\dagger}c_n|\Phi\rangle$ we also have the pairing tensor $\hat{\kappa}_{nn'} = \langle\Phi|c_{n'}c_n|\Phi\rangle$ and the total energy density functional now contains a pairing term

$$E_{RHB}[\hat{\rho}, \hat{\kappa}] = E_{RMF}[\hat{\rho}] + E_{pair}[\hat{\kappa}], \tag{8}$$

which is determined by the specific type of pairing interaction. In the current study a finite range pairing force, which is a modified version of the Gogny pairing force has been used [4, 5] typically referred as TMR force. In coordinate space it has the form of a two body force

$$V(\mathbf{r}_1, \mathbf{r}_2, \mathbf{r}_1', \mathbf{r}_2') = -G\delta(\mathbf{R} - \mathbf{R}')P(r)P(r')\frac{1}{2}(1 - P^{\sigma}), \qquad P(r) = \frac{1}{(4\pi a^2)^{3/2}} e^{-\frac{r^2}{4a^2}}. \tag{9}$$

Presently, the strength parameter G has been adjusted at each isotope so that it reproduces the experimental pairing gap as defined by the three point indicator. For the neutron channel it has the form

$$\Delta^{(3)}(N) = \frac{(-1)^N}{2}(2BE(Z,N) - BE(Z,N-1) - BE(Z,N+1)), \tag{10}$$

and equivalently for protons.

A variation of the energy density functional with respect to both particle and pairing densities leads to the RHB matrix equations

$$\begin{pmatrix} \hat{h}_D - m - \lambda & \hat{\Delta} \\ -\hat{\Delta}^* & -\hat{h}_D + m + \lambda \end{pmatrix} \begin{pmatrix} U_k(\mathbf{r}) \\ V_k(\mathbf{r}) \end{pmatrix} = E_k \begin{pmatrix} U_k(\mathbf{r}) \\ V_k(\mathbf{r}) \end{pmatrix}, \tag{11}$$

where we have two average potentials, the Dirac field given by the variation of the energy functional with respect to the particle density

$$\hat{h}_D = \frac{\delta E}{\delta \hat{\rho}}, \tag{12}$$

and the pairing field obtained from the variation of the energy functional with respect to the pairing tensor

$$\hat{\Delta} = \frac{\delta E}{\delta \hat{\kappa}}. \tag{13}$$

The numerical diagonalisation of the RHB matrix yields the Bogoliubov wavefunctions U and V as well as the quasiparticle energies E_k. In practice, once these are obtained one can calculate any observable in the static picture of the ground state of a nucleus.

2.2 Collective Hamiltonian

To calculate excitation spectra and transition probabilities for quadrupole vibrations and rotations, it is necessary to restore the collective correlations and symmetries broken by the mean-field approximation. The formal method for achieving this is the Generator Coordinate Method (GCM). This involves using the results of constrained Relativistic Hartree-Bogoliubov (RHB) calculations and then projecting the total wavefunction onto states with good quantum numbers (like angular momentum and parity). However, this GCM approach is computationally demanding, especially for heavy nuclei. A common alternative is to use the constrained RHB results to map the energy surface. This surface is then used as input to construct a simpler, effective collective Bohr-type Hamiltonian, which is less computationally intensive while still capturing the essential collective dynamics.

$$H_{coll} = T_{vib}(\beta,\gamma) + T_{rot}(\beta,\gamma,\Omega) + V_{coll}(\beta,\gamma). \tag{14}$$

The three terms of the Hamiltonian are:

- the vibrational kinetic energy $T_{vib} = \frac{1}{2}B_{\beta\beta} + \beta B_{\beta\gamma}\dot{\beta}\dot{\gamma} + \frac{1}{2}\beta^2 B_{\gamma\gamma}\dot{\gamma}^2$
- the rotational kinetic energy $T_{rot} = \frac{1}{2}\sum_{k=1}^{3} I_k \omega_k^2$
- and the collective potential $V_{coll}(\beta\gamma) = E_{rot}(\beta\gamma) - \Delta V_{vib}(\beta\gamma) - \Delta V_{rot}(\beta\gamma)$.

The entire dynamics of the collective Hamiltonian is governed by seven functions of the intrinsic deformations β, γ and the three Euler anglesΩ: the three mass parameters $B_{\beta\beta}$, $B_{\beta\gamma}$, $B_{\gamma,\gamma}$, the three moments of inertia I_k and the collective potential.

3. Results and Discussion

3.1 Mean-field results

The first step of this investigation is to solve the RHB equations (11) for each nucleus on the isotopic chains of Er and Yb with $82 < N < 114$. The specific relativistic Lagrangian employed is given by the parameter set of DD-ME2 [6], that is a meson exchange interaction with density dependent coupling constants, along the TMR pairing force. The self-consistency of the solution is based on the variation method through an iteration procedure that ensures the minimization of the energy with respect to changes in the densities. This gives an approximation of the static ground state of the nucleus.

A more evolved approach is to apply certain constraints on the values of operators that are related to the shape of a nucleus. The most common and the ones we used are the quadrupole operators, $\hat{Q}_{20} = 2z^2 - x^2 - y^2$ and $\hat{Q}_{22} = x^2 - y^2$ since they describe the basic shapes found in nuclei, spherical, axially deformed or triaxial deviations. Consequently the average energy is minimized with the additional condition of the operators having a certain value i.e.

$$\langle\hat{H}\rangle + \sum_{\mu=0,2} C_{2\mu}\left(\langle\hat{Q}_{20}\rangle - q_{2\mu}\right)^2. \tag{15}$$

Typically, quadrupole shapes of nuclei are characterized by the Hill-Wheeler β and γ coordinates which are defined from the relations:

$$Q_{20} = \beta\cos\gamma, \qquad Q_{22} = \frac{1}{\sqrt{2}}\beta\sin\gamma. \tag{16}$$

The β coordinate gives the axial elongation. So for $\beta = 0$ the shape is spherical, and for $\beta \approx 0.2 - 0.3$ the shape is axially deformed. In that case if $\gamma = 0^o$ the nucleus is prolate and if $\gamma = 60^o$ the nucleus is oblate. For in between values of γ there is also a triaxial degree of freedom.

The constrained RHB calculations are performed over a discrete mesh of points in the polar plane of the β and γ coordinates, where β goes from 0 to 0.6 with a step of 0.05 and γ from 0^o to 60^o with a 10^o step. This allows us to plot the projected energy surface PES on that specific plane. The point with the lowest energy corresponds to the ground state. We are thus able to examine how the shape of each isotope changes in the mean-field level.

In Fig. 1 we show the PESs for Er isotopes with $82 < N < 104$. The ground state corresponds to the dark blue area. Naturally, the first isotopes ^{150}Er and ^{152}Er that are close to the $N = 82$ magic number, have a minimum at the $\beta = 0$, $\gamma = 0^o$ point i.e. they are spherical. As the neutron number increases the respective isotopes become more deformed, as the minimun moves to the right of the $\gamma = 0$ axis. In particular, beyond ^{156}Er all isotopes possess a clear prolate shape with axial deformation $0.2 < \beta < 0.35$. Note that based on the PES ^{154}Er can be identified as transitional and actually its minimum lies in the triaxial region. Another typical characteristic as the neutron number increases is the narrowing of the blue area around the minimum. Meaning that, the isotopes become more rigid and less sensitive to triaxial vibrations. In Fig. 2 the respective projected energy surfaces are

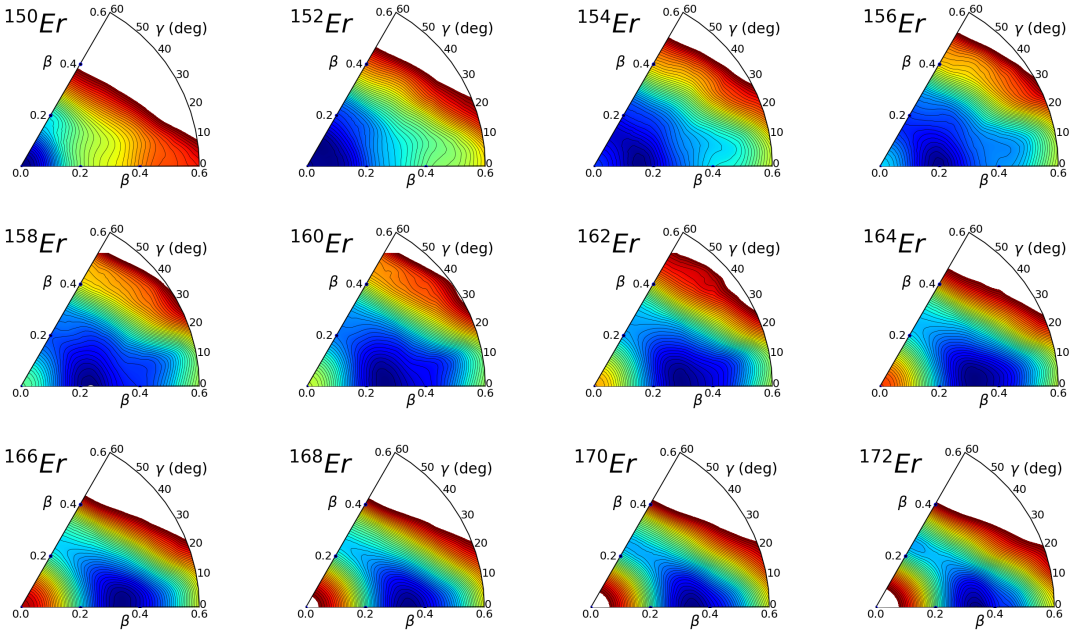

Figure 1. Projected energy surfaces of Er isotopes with $82 < N < 104$, from constrained RHB calculations with the DD-ME2 Lagrangian and the TMR pairing force.

shown for the same neutron numbers but now for Yb isotopes. Practically the overall picture is identical to that of Er isotopes. Only minor differences are observed in the position of the ground state minimum and the size of region with low energies around it.

3.2 Collective Hamiltonian results

In the second part of the study we concentrated our analysis on the collective behavior of Yb isotopes, in order to compare with our recent experimental results. For this we use the collective Hamiltonian

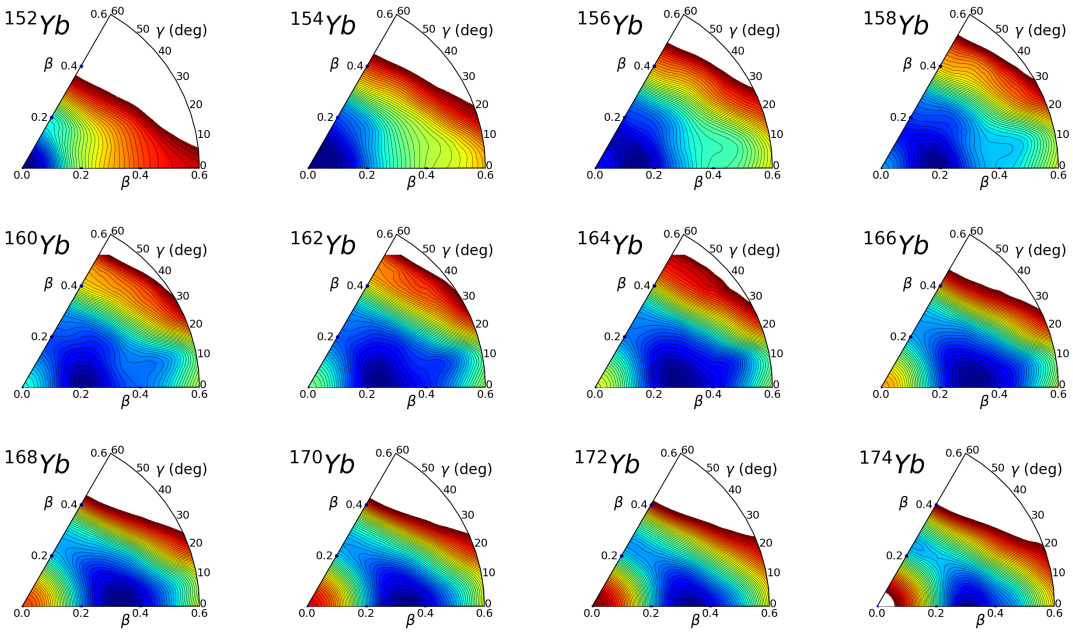

Figure 2. Same as Fig. 1 but for Yb isotopes with $82 < N < 104$.

of eq.(14) in the five dimensions- (5DCH) of β, γ and the three Euler angles Ω, which is an approximation beyond the relativistic mean-field [8]. The parameters of the Hamiltonian are completely determined by the constrained RHB calculations. Specifically at each point in the PES, the mass parameters $B_{\beta\beta}$, $B_{\beta\gamma}$, $B_{\gamma,\gamma}$, are calculated within the cranking approximation and the three moments of inertia I_k are calculated using the Inglis-Belyaev formula. The collective Hamiltonian is then derived in the Gaussian overlap approximation [9]. In this way we are able to extend the fully microscopic approach to a collective model that can describe quadrupole rotations and vibrations. The numerical diagonalisation of the Hamiltonian is equivalent with the solution of the corresponding eigenvalue problem. In the end we get the eigenvalues and eigenfunctions of the Hamiltonian,

$$\Psi_a^{IM}(\beta,\gamma,\theta) = \sum_{K\in\Delta I} \Psi_{aK}^{I}(\beta,\gamma)\Phi_{MK}^{I}(\theta), \tag{17}$$

in other words the complete spectrum of the quadrupole rotational and vibrational excited states. I is the total angular momentum of each state and M and K are its projections on the laboratory and intrinsic third axis respectively. A typical spectrum of low-lying excited states contains the ground state band with its excited states built above and several other bands. Their structure and position can lead to their identification as β or γ bands. A way to determine the band type where each state belongs is by examining its K component. Excited states with predominant $K = 2$ components belong to a γ band, while states with predominant $K = 0$ belong to the β band above the yrast states that usually belong to the ground state band. Fig.3 shows exactly the distribution of the K components for the states 2_2^+, 2_3^+, 4_2^+ and 4_3^+, for the first five Yb isotopes. The isotopes ^{154,156,158}Yb that are near the spherical closure at $N = 82$ present significant mixing. However, as they approach the rigid rotor limit they include pure rotational and vibrational states. Based on that fact we can assign the calculated states to the right band.

An insightful figure is to plot the evolution of the systematics of states, characterized by I^π, belonging to a band along the isotopic chain. In Figs. 4 and 5 we have plotted the systematic change of the

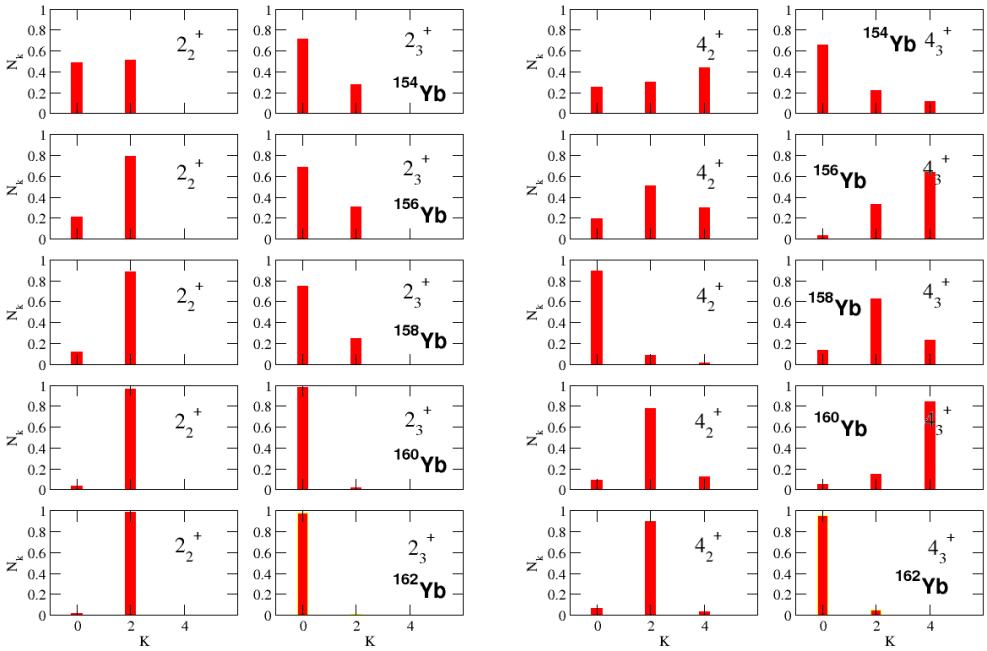

Figure 3. Distribution of the K components in the collective wavefunctions. Left figure 2_2^+ and 2_3^+ states, right figure 4_2^+ and 4_3^+ states

ground state band and the (quasi-) gamma band. The choice, was based on the fact that there are available experimental data in the ENSDF database [10]. In each figure the left diagram shows the theoretical results and the right diagram the evaluated experimental energies. Based on the previous analysis of the PESs there is also at each diagram a delineation of the γ-soft and rigid rotor regions of the Yb isotopic chain. Clearly isotopes with $86 \leq N \leq 92$ that we can place at the near- spherical transitional type, show larger distance between intraband states. Isotopes that can be associated with a rigid rotor with $N \geq 94$ have an approximately flat behavior.

For the ground state band these isotopes follow the $I(I+1)$ pattern. There is rather good agreement of the theoretical calculations with the experimental energies, especially in the rigid rotor region. Larger deviations are observed near the $N = 82$ closure, where the particular model in principle shows limited success.

For the (quasi-) gamma band we also calculate a systematic decrease of all the energies up to $N = 92$ where the end of the γ-soft region is. Interestingly, the observed states show a kink with a maximum at $N = 104$ which is the middle of the neutron shell. This indicates that the particular isotope is more rigid against γ vibration compared to its neighbors. Theoretically, this can be explained by the PESs where as we saw, the whole surface becomes narrower around the minimum and especially stiff along the γ direction. In the collective Hamiltonian results we do see a slight increase from $N = 92$ and onwards, but generally the excited states stay rather flat.

Other useful spectroscopic quantities are certain energy ratios that also reveal the collective behavior of each isotope. Two of the most commonly used are the ratio $R_{4/2} = E_{4_1^+} - E_{2_1^+}$ of the first 4_1^+ excited state over the first 2_1^+ and $R_{6/2} = E_{6_1^+} - E_{2_1^+}$ of the first 6_1^+ over again 2_1^+. These are presented in Fig. 6 for the results obtained with DD-ME2, together with the values from the experimental energies [10] and the result of the recent experiment on ^{178}Yb by Koseoglou et. al. to be published. Within

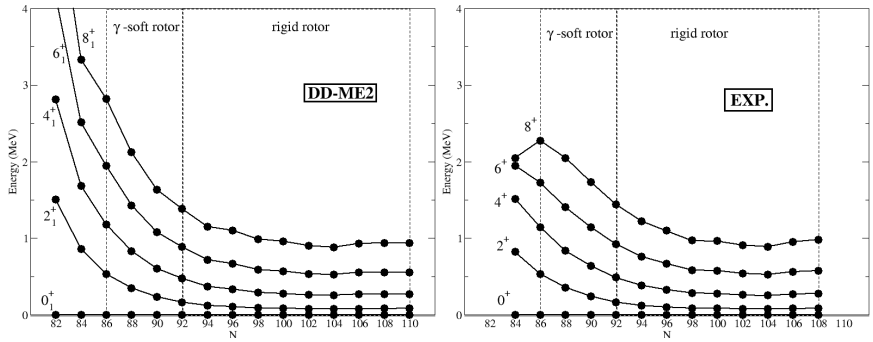

Figure 4. Evolution of the ground state band excited states with increasing N. The left figure are the theoretical results, the right figure are the experimentally assigned energies.

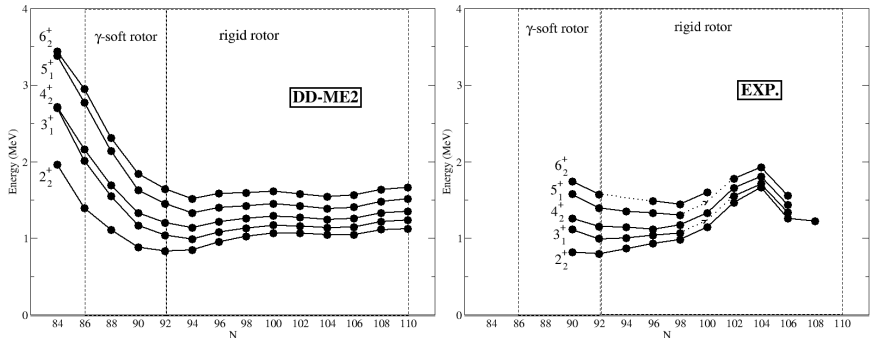

Figure 5. Same as Fig. 4 but for the (quasi-) gamma band

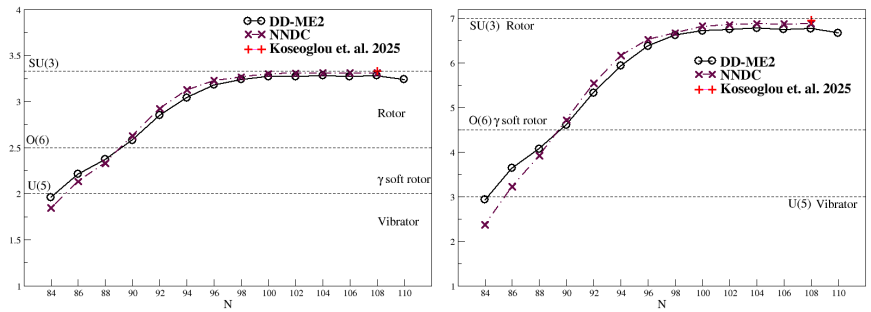

(a) $R_{4/2}$ **(b)** $R_{6/2}$

Figure 6. $R_{4/2}$ and $R_{6/2}$ energy ratios from 5DCH based on DD-ME2, experimantal values from [10] and the value for ^{178}Yb from Koseoglou et. al.

each subfigure we also designate the corresponding values for the two ratios as they are determined by the underlying dynamical symmetry of the Interacting Boson Model. At first glance there is a nice agreement of the theory with experiment. Both quantities reaffirm the previous conclusions. First, that isotopes with $84 \leq N \leq 92$ can be placed in the transitional region of γ-soft nuclei. Second that isotopes with $N > 94$ are at the rigid rotor region, with $^{170-178}$Yb being practically perfect rotors. Notably the maximum value for both ratios is obtained for ^{178}Yb, where the recent results by Koseoglou et. al. give slightly larger value than ENSDF [10]. Finally, in Fig. 7 we plot

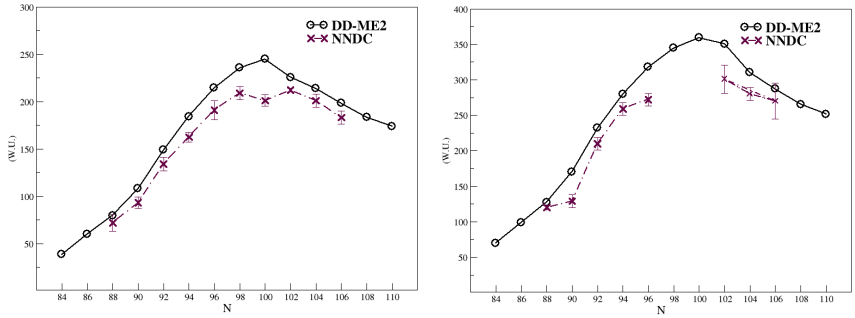

(a) $B(E2; 2_1^+ \rightarrow 0_{gs}^+)$ **(b)** $B(E2; 4_1^+ \rightarrow 2_1^+)$

Figure 7. Quadrupole transition probabilities from 5DCH based on DD-ME2 and experimantal values from [10]

the theoretically calculated quadrupole transition probabilities $B(E2; 2_1^+ \rightarrow 0_{gs}^+)$ and $B(E2; 4_1^+ \rightarrow 2_1^+)$ and their experimental values [10]. These observables are also crucial as a measure of collectivity the higher they are. Furthermore, they provide an indirect estimate of the quadrupole deformation β_2 in the case of a rigid rotor isotope. There is a reasonable agreement of the theoretical model with the overall experimantal trend. As expected transition probabilities have relatively low values near $N = 82$, and gradually increase to a maximum located at $N = 100$ (^{170}Yb) before they start decreasing for $N \geq 102$. Interestingly, the experimental $B(E2; 2_1^+ \rightarrow 0_{gs}^+)$ has a small dip at $N = 100$ (^{170}Yb) instead of a maximum.

4. Conclusion

In the present contribution, the relativistic energy density functional framework, extended beyond the mean-field level through a five-dimensional Collective Hamiltonian (5DCH), was successfully applied to investigate the shape transition and collective properties of Er and Yb isotopic chains ($82 < N < 114$). The analysis, starting from projected potential energy surfaces (PESs) calculated with the DD-ME2 parameter set, clearly illustrated the transition from spherical to γ-soft to well-deformed prolate shapes as the neutron number increased. The subsequent diagonalization of the 5DCH provided microscopic descriptions of the low- lying excitation spectra and transition probabilities. Key findings, such as the evolution of band energies and the critical energy ratios $R_{4/2}$ and $R_{6/2}$, demonstrated excellent agreement with available experimental data, firmly establishing the presence of a transitional γ-soft region ($84 \leq N \leq 92$) and a robust rigid rotor region ($N \geq 94$). While some larger deviations were observed near the $N = 82$ magic number, the overall performance of RHB+5DCH framework validates its use for systematically studying collectivity in the rare-earth region, and paves the way for future studies incorporating additional degrees of freedom or examining shape coexistence phenomena in neighboring nuclei.

5. Acknowledgments

The calculations were performed at the NuSTRAP (Nuclear Structure, Reactions & Applications - https://radium.phys.uoa.gr/nustrap) computational facilities in the National and Kapodistrian University of Athens. PK was funded by the Deutsche Forschungsgemeinschaft (DFG, German Research Foundation) – 539757749.

References

[1] P. Ring. "Relativistic mean field theory in finite nuclei". In: *Prog. Part. Nucl. Phys.* 37 (1996), pp. 193–263. ISSN: 0146-6410. DOI: 10.1016/0146-6410(96)00054-3.

[2] B. D. Serot. "A relativistic nuclear field theory with pi and rho mesons". In: *Phys. Lett. B* 86.2 (1979), pp. 146 –150. ISSN: 0370-2693. DOI: 10.1016/0370-2693(79)90804-9.
[3] B. D. Serot and J. D. Walecka. "The relativistic nuclear many-body problem". In: *Adv. Nucl. Phys.* 16 (1986). Ed. by J. W. Negele and E. Vogt, pp. 1–327.
[4] Y. Tian, Z. Y. Ma, and P. Ring. "A finite range pairing force for density functional theory in superfluid nuclei". In: *Phys. Lett. B* 676 (2009), p. 44. DOI: 10.1016/j.physletb.2009.04.067. eprint: 0908.1844.
[5] Y. Tian, Z. Y. Ma, and P. Ring. "Separable Pairing Force for Relativistic Quasiparticle Random Phase Approximation". In: *Phys. Rev. C* 79 (2009), p. 064301. DOI: 10.1103/PhysRevC.79.064301. eprint: 0908.1845.
[6] G. A. Lalazissis, T. Nikšić, D. Vretenar, and P. Ring. "New relativistic mean field interaction with density dependent meson couplings". In: *Phys. Rev. C* 71 (2005), p. 024312. DOI: 10.1103/PhysRevC.71.024312.
[7] T. Nikšić, N. Paar, D. Vretenar, and P. Ring. "DIRHB - a relativistic self-consistent mean-field framework for atomic nuclei". In: *Comp. Phys. Comm.* 185.6 (2014), pp. 1808 –1821. ISSN: 0010-4655. DOI: 10.1016/j.cpc.2014.02.027. eprint: 1403.4039.
[8] T. Nikšić, Z. P. Li, D. Vretenar, L. Prochniak, J. Meng, and P. Ring. "Beyond the relativistic mean-field approximation. III. Collective Hamiltonian in five dimensions". In: *Phys. Rev. C* 79 (3 2009), p. 034303. DOI: 10.1103/PhysRevC.79.034303. eprint: 0811.0233.
[9] P. Ring and P. Schuck. *The Nuclear Many-Body Problem*. Berlin: Springer-Verlag, 1980.
[10] National Nuclear Data Center. *Evaluated Nuclear Structure Data File (ENSDF)*. https://www.nndc.bnl.gov/ensdf/. Accessed: April 15, 2025.